Stem Cell Reports
Article

ISSCR

OPEN ACCESS

The global downregulation of protein synthesis observed during hepatogenic maturation is associated with a decrease in TOP mRNA translation

Marino Caruso,[1] Sébastien Meurant,[1] Damien Detraux,[1] Amandine Mathieu,[1,2] Manon Gilson,[1] Marc Dieu,[3] Antoine Fattaccioli,[1] Catherine Demazy,[1,3] Mustapha Najimi,[2] Etienne Sokal,[2] Thierry Arnould,[1] Catherine Verfaillie,[4] Denis L.J. Lafontaine,[5] and Patricia Renard[1,2,*]

[1]Laboratory of Biochemistry and Cell Biology (URBC), Namur Research Institute for Life Sciences (NARILIS), University of Namur (UNamur), Namur, Belgium
[2]Laboratory of Pediatric Hepatology and Cell Therapy, Institut de Recherche Clinique et Expérimentale (IREC), Catholic University of Louvain, Brussels, Belgium
[3]Mass Spectrometry Facility (MaSUN), University of Namur, Namur, Belgium
[4]Department of Development and Regeneration, Stem Cell Institute, KU Leuven, Leuven, Belgium
[5]RNA Molecular Biology, Fonds de la Recherche Scientifique (FRS/FNRS), Université Libre de Bruxelles (ULB), Biopark Campus, Gosselies, Belgium
*Correspondence: patsy.renard@unamur.be
https://doi.org/10.1016/j.stemcr.2022.11.020

SUMMARY

Translational regulation is of paramount importance for proteome remodeling during stem cell differentiation at both the global and the transcript-specific levels. In this study, we characterized translational remodeling during hepatogenic differentiation of induced pluripotent stem cells (iPSCs) by polysome profiling. We demonstrate that protein synthesis increases during exit from pluripotency and is then globally repressed during later steps of hepatogenic maturation. This global downregulation of translation is accompanied by a decrease in the abundance of protein components of the translation machinery, which involves a global reduction in translational efficiency of terminal oligopyrimidine tract (TOP) mRNA encoding translation-related factors. Despite global translational repression during hepatogenic differentiation, key hepatogenic genes remain efficiently translated, and the translation of several transcripts involved in hepatospecific functions and metabolic maturation is even induced. We conclude that, during hepatogenic differentiation, a global decrease in protein synthesis is accompanied by a specific translational rewiring of hepatospecific transcripts.

INTRODUCTION

Cell differentiation can be regarded as when the stem cell proteome needs to be remodeled to support acquisition of the new functions of differentiated cells. Different mechanisms can contribute to defining the cell proteome, including epigenetic regulation, transcription control, regulation of mRNA stability, translation efficiency, and regulation of protein stability (Vogel and Marcotte, 2012). Therefore, considerable efforts have been invested in understanding better how these mechanisms participate in stem cell differentiation, with a particular emphasis on transcription. More particularly, in the context of hepatogenic differentiation, transcription factors governing differentiation have been extensively characterized in the past years, allowing a better understanding of the gene-regulatory network(s) controlling differentiation (reviewed in Gérard et al., 2017). However, multiple "omic" studies have demonstrated that the correlation between transcript and protein abundance can be extremely variable in different biological contexts (Liu et al., 2016; Schwanhüusser et al., 2011). This highlights the importance of post-transcriptional regulation mechanisms such as translational regulation.

Proteomic remodeling is considered to be largely determined by transcriptomic modifications in steady-state conditions, while translational regulation offers a faster regulatory mechanism allowing rapid proteomic remodeling to respond to external and internal stimuli during highly dynamic biological processes such as cell differentiation (Liu et al., 2016; Tahmasebi et al., 2019). This is further supported by reports demonstrating the impact of cell differentiation on protein synthesis (Kristensen et al., 2013; Lu et al., 2009). These observations, linking translational control and stem cell fate, prompted several teams to study both specific and global translational regulation mechanisms during stem cell differentiation (reviewed in Gabut et al., 2020; Tahmasebi et al., 2019). First, at the transcript-specific level, translation of C-MYC and NANOG has been shown to be regulated by EIF2α through an upstream open reading frame (uORF)-mediated translational regulation during pluripotency maintenance or exit (Friend et al., 2015). Translational regulation of YY2 (Yin-Yang 2), a transcription factor involved in the control of POU5F1 (POU domain, class 5, transcription factor 1, also known as OCT4) expression, participates in the control of embryonic stem cell (ESC) pluripotency and self-renewal (Tahmasebi et al., 2016). In addition, at the global level, protein synthesis rate is connected with pluripotency exit and differentiation: increased translation is indeed observed upon ESC transition toward differentiated progeny (Easley et al., 2010; Guzzi et al., 2018; Sampath et al., 2008). However, contradictory reports by You and collaborators showed a global protein synthesis decrease upon mouse

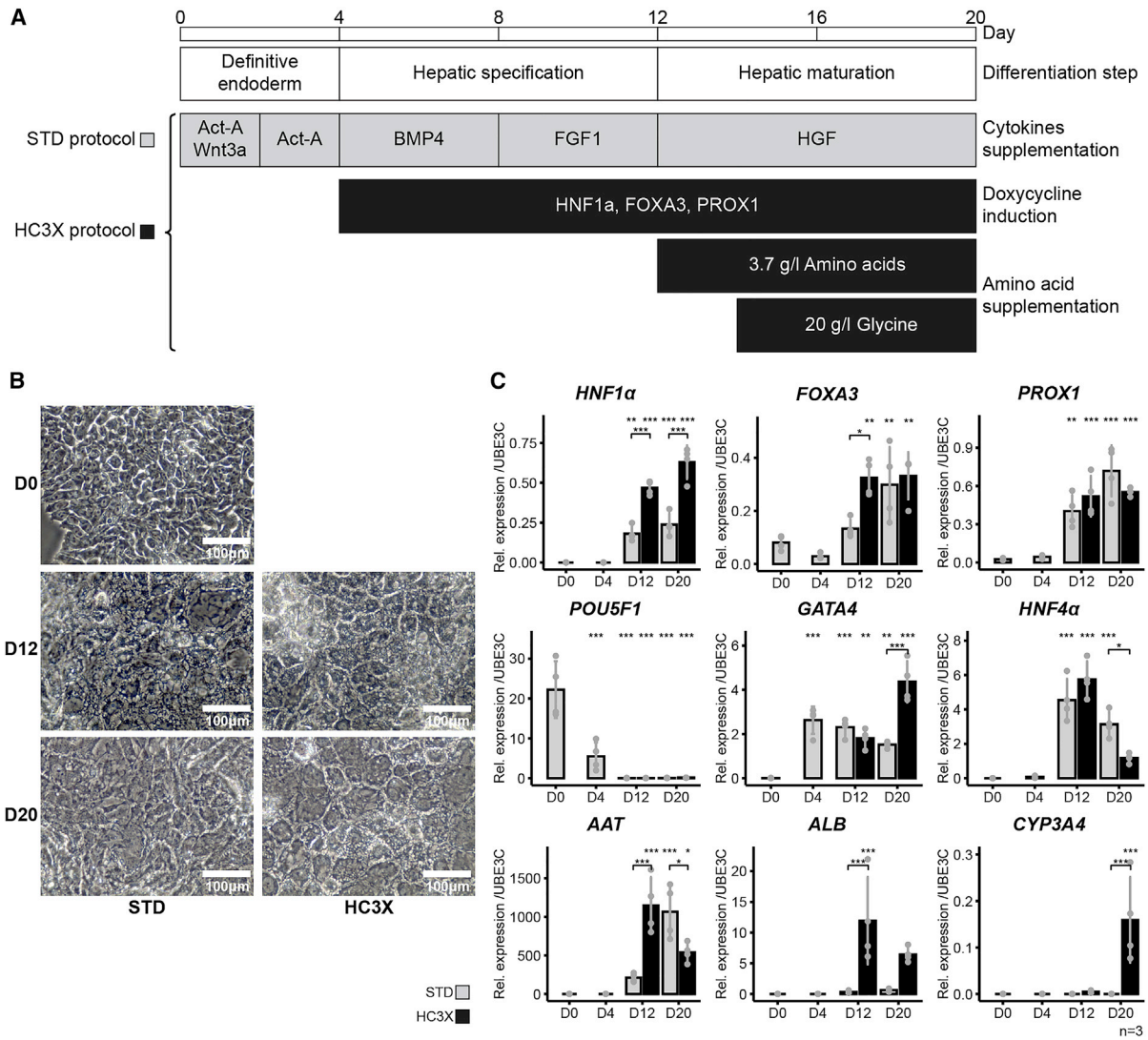

(legend on next page)

ESC differentiation (You et al., 2015). This downregulation of global translation is further supported by the repression of ribosome biogenesis occurring in differentiating cells, as shown by downregulation of ribosomal protein translation upon embryoid body (EB) differentiation (Ingolia et al., 2011) or decrease in rRNA synthesis upon human (h) ESC differentiation induction by a 48-h activin A treatment (Woolnough et al., 2016). Importantly, these results are restricted to pluripotency exit rather than acquisition of a mature differentiated cell phenotype, as, for instance, during EB differentiation only early events of embryogenesis are recapitulated, yielding progeny expressing markers of the three germ layers but not yet mature cell markers (Zeevaert et al., 2020). Therefore, the relevance of these mechanisms in the acquisition of the proteome corresponding to that of a terminally differentiated cell remains to be established, and investigations concerning a potential translational mechanism participating in hepatogenic maturation are currently lacking.

In this study, we took advantage of a recently published *in vitro* hepatogenic differentiation protocol for induced pluripotent stem cells (iPSCs) yielding hepatocyte-like cells (HLCs) presenting a maturity phenotype closer to freshly isolated hepatocytes (Boon et al., 2020). Using this optimized but also a standard protocol and polysome profiling, we aimed at characterizing the translational reprogramming occurring during hepatogenic differentiation to evaluate the relative contribution of translation to the acquisition of a maturing hepatocyte proteome.

RESULTS

Models of hepatogenic differentiation

For hepatocyte differentiation, we used two different protocols. In the first protocol, we applied the methods described in Roelandt et al. (2013) (Figure 1A), which we will name the "standard" (STD) protocol. In this scheme, we used successive treatments with cytokine cocktails driving definitive endoderm formation, hepatic specification, and hepatic maturation after 4, 12, or 20 days of differentiation, respectively. This protocol induces differentiation of pluripotent stem cells toward HLCs expressing key hepatogenic transcription factors and functional markers as well as susceptibility to hepatotropic virus infections (Tricot et al., 2018). A second protocol consisted of an improved differentiation scheme in which PSCs undergo genetic engineering (doxycycline induction of three hepatic transcription factors [HNF1A, FOXA3, and PROX1]) from day 4 of differentiation (termed HC3X cells) and differentiation is further optimized by metabolic engineering of the culture medium (supplementation of 3.7 g/L amino acid cocktail from day 12 of differentiation and 20 g/L glycine from day 14 of differentiation) (Figure 1A) (Boon et al., 2020). The HC3X protocol yields HLCs presenting a maturity phenotype closer to freshly isolated hepatocytes in terms of both metabolic activity and hepatocyte-specific functions, as demonstrated by the detection of comparable albumin (*ALB*) mRNA levels or by measurement of glucose uptake/secretion and 7-benzyloxy-4-trifluoromethylcoumarin (BFC) metabolic assays (Boon et al., 2020).

In our study, the differentiation of iPSCs toward HLCs was systematically evaluated by phase-contrast microscopy and qRT-PCR assays for specific mRNA markers (Figures 1B and 1C). For the STD and HC3X protocols, the acquisition of the typical hepatocyte polygonal-shaped cell morphology was confirmed on day 20 of differentiation (Figure 1B). HC3X protocol progeny showed increased cell size and cell border definition compared with cells that underwent the STD protocol. The loss of the pluripotency marker *POU5F1* and induction of definitive endoderm and hepatic transcripts *GATA4* and *HNF4A* (from days 4 and 12 of differentiation, respectively) were also confirmed (Figure 1C). As

Figure 1. Models of hepatogenic differentiation

(A) Schematic representation of culture protocols showing the three steps of *in vitro* hepatogenic differentiation. For the STD hepatogenic differentiation protocol, iPSCs were sequentially treated with corresponding cytokines for a total of 20 days. For the HC3X hepatogenic differentiation protocol, standard differentiation medium was supplemented with doxycycline to induce expression of HNF1A, FOXA3, and PROX1 from D4 of differentiation and with amino acids from D12 and D14 of differentiation. For the majority of experiments, control cells were harvested at D0 and differentiating cells (with STD or HC3X protocol) were harvested at D12 and D20.

(B) Phase-contrast micrographs illustrating the morphological changes occurring during hepatogenic differentiation of iPSCs (scale bars, 100 μm).

(C) qPCR analysis showing the relative mRNA abundance of key differentiation markers during hepatogenic differentiation of iPSCs. Induced hepatic transcription factors (*HNF1A*, *FOXA3*, *PROX1*), a pluripotency marker (*POU5F1*), differentiation markers (*GATA4*, *HNF4A*), and hepatic functional markers (*ALB*, *AAT*, *CYP3A4*) are shown. Results are normalized on ubiquitin-protein ligase E3C (*UBE3C*) and plotted as mean ± SD of four independent biological replicates. Statistical significance was calculated by ANOVA and Tukey's HSD *post hoc* test. *$p < 0.05$, **$p < 0.01$, and ***$p < 0.001$.

(D and E) Ontology analysis of proteomic data. Log2 fold changes in protein abundance obtained by label-free quantitative proteomics were used to produce a ranked protein list analyzed by GSEA using GO biological process and KEGG annotation databases. Normalized enrichment scores of selected upregulated and downregulated terms for both STD and HC3X protocols at two time points, D12 (D) and D20 (E) compared with D0 are shown (terms with $p < 0.05$ were considered significantly enriched).

expected, the progressive increase in *HNF1A*, *FOXA3*, and *PROX1* transcript abundance observed in the STD protocol was further enhanced by doxycycline induction of these transgenes from day 4 in HC3X differentiation. In addition, while expression of the hepatic functional marker α1 antitrypsin (*AAT*) was significantly induced in both protocols, only HC3X progeny showed strong induction of *ALB* and cytochrome P450 3A4 (*CYP3A4*) transcripts. Globally, the markers analyzed by qRT-PCR in differentiated cells showed a similar pattern of expression by comparison to freshly isolated hepatocytes (data not shown, and see Boon et al., 2020, for details).

Next, we analyzed differentiating cells by label-free mass spectrometry to establish the acquisition of a hepatogenic phenotype at the protein level. Log2 fold change (Log2FC) of protein abundance in control day 0 (D0) iPSCs versus differentiated cells at D12 (Figure 1D) or D20 (Figure 1E) for cells undergoing either the STD or the HC3X protocol was used for gene set enrichment analysis (GSEA) (see complete list of results in Table S1). At the end of hepatic specification (D12), the data showed a significant positive enrichment of several gene ontology (GO) biological process and KEGG pathway terms linked to lipid and carbohydrate metabolism, indicative of metabolic maturation. We also found hepatic-specific groups of enriched terms linked to glycogen metabolism, plasma protein secretion, and cellular detoxification. Finally, relevant terms in the context of hepatogenic differentiation such as cholesterol metabolism and transmembrane transport were also significantly enriched. For both comparisons between control iPSCs and differentiated cells at D12 or D20, we found negative enrichment of terms related to cell cycle and, interestingly, to protein synthesis, including numerous ribosomal proteins.

These results confirm that iPSCs were successfully guided toward hepatogenic differentiation in the STD and HC3X protocols as shown by the induction of key hepatogenic transcription factors and acquisition of the hepatocyte morphological phenotype. In addition, HC3X progeny acquire a greater hepatic maturation, as shown by higher expression of functional hepatocyte markers, as previously described (Boon et al., 2020). Perhaps more unexpectedly, proteomic analysis of differentiating cells indicated a decrease in abundance of many components of the protein synthesis machinery during hepatogenic differentiation.

Hepatogenic maturation induces a global decrease in protein synthesis rate

As proteomic analysis revealed a negative enrichment for several proteins related to the translation machinery, we next aimed to characterize global protein synthesis during iPSC differentiation using a puromycin-incorporation assay (Figure 2A). Western blot analysis of puromycin-labeled peptides showed a biphasic profile along the differentiation process: the global protein synthesis is first strongly and highly significantly upregulated after 2 days of differentiation, corresponding to endodermal lineage commitment. It then progressively decreases to levels inferior to undifferentiated iPSCs (D0): after 20 days of differentiation with the STD or HC3X protocol, the translation rate reached 32% and 42% of D0, respectively. This transient upregulation of protein synthesis is in line with several reports focusing on the early steps of differentiation (such as EB formation; Sampath et al., 2008) and demonstrating an increase in protein synthesis upon PSC differentiation (reviewed in Gabut et al., 2020; Tahmasebi et al., 2019). However, this is the first time that a subsequent decrease in global protein synthesis occurring during hepatogenic maturation is described.

These results thus indicate a two-step process of global translational regulation, where early stimulation of protein synthesis is followed by a global repression of translation during hepatogenic maturation.

The global translation profile was further characterized by polysomal analysis in undifferentiated iPSCs and differentiating cells (Figure 2B). Polysomal analysis consists in the fractionation of cellular lysates in sucrose density gradient followed by measurement of absorbance at 254 nm along the gradient. This allows us to establish the distribution profiles of ribosomal 40S and 60S subunits, 80S monosomes, and polysomes, which is a means to assess global translation. The data show that at D12 and D20, differentiated cells undergoing either the STD or the HC3X protocol display an increased 80S peak associated with reduced polysomes, indicating a global reduction of translation.

In conclusion, using two models of hepatogenic differentiation, our data confirm a previously described upregulation of translation during pluripotency exit, but it also reveals that this effect is transient and that the increased protein translation phase is followed by a global reduction of translation during hepatogenic maturation. Importantly, this conclusion was correlated with a decreased abundance of components of the translational machinery observed by proteomic analysis (Figures 1C and 1D; negative enrichment).

Characterization of translational regulation during differentiation

The global downregulation of protein synthesis observed upon hepatogenic differentiation was quite unexpected, since hepatocytes are generally considered as "biochemical factories" actively involved in multiple metabolic pathways and dedicated to plasma protein production. A polysome profiling experiment was thus used to characterize the specific translational reprogramming occurring during differentiation. Polysome profiling is a technique to measure mRNA translation by RNA-sequencing (RNA-seq)

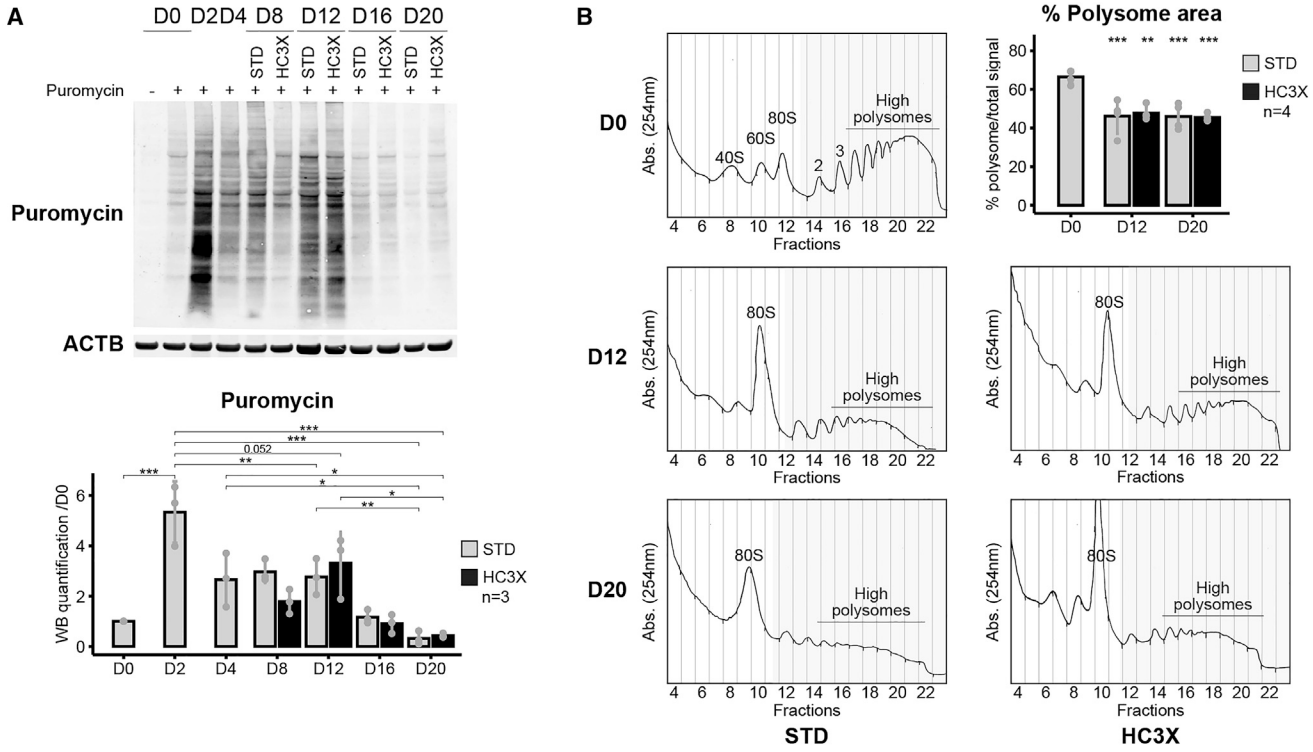

Figure 2. Hepatogenic differentiation induces a global decrease in protein synthesis rate

(A) Western blot analysis of puromycin-incorporated nascent polypeptides in control iPSCs and differentiating cells at days 2, 4, 8, 12, 16, and 20. iPSCs left untreated by puromycin were used as control (top). Western blot signal intensity was quantified and normalized over β-actin (ACTB) signal and plotted as mean ± SD of three independent replicates (bottom). Statistical significance was calculated by ANOVA and Tukey's HSD *post hoc* test (significance is shown comparing only D0, D2, D12 STD, D12 HC3X, D20, and D20 HC3X). *$p < 0.05$, **$p < 0.01$, and ***$p < 0.001$.

(B) Polysome fractionation profile during differentiation. Ribosomal subunits (40S and 60S), monosomes (80S), and polysomes from control D0 iPSCs or differentiating cells at D12 or D20 with STD and HC3X protocols were separated on a sucrose density gradient and fractionated into 24 fractions. Graphs show absorbance at 254 nm along the sucrose gradient and are representative of four biological replicates. Polysomal signal in the gradient is colored in gray. Bar plot represents mean ± SD of percentage of polysomal signal calculated by normalizing the polysomal area under the curve by total area under the curve for four independent biological replicates. Statistical significance was calculated by ANOVA and Tukey's HSD *post hoc* test.

analysis of efficiently translated mRNA (i.e., mRNAs with >3 bound ribosomes, called hereafter "high polysomes"; HP) (Figure 3A) (Gandin et al., 2014). anota2seq analysis of RNA-seq data quantifies the log2 translational efficiency fold change (Log2TE FC) of mRNAs and integrates mRNA abundance regulation and translational regulation to assign each mRNA to a regulatory mode: "translation" (modified mRNA abundance in the HP samples that is not paralleled by corresponding total mRNA levels), "buffering" (opposite modification of mRNA abundance in HP and total RNA), "abundance" (similar modifications of mRNA abundance in HP and total RNA), or "background" (mRNA abundance modified neither in HP nor in total RNA) (Oertlin et al., 2019).

For each comparison between D0 control iPSCs and D12 or D20 differentiating cells, a scatterplot of Log2FC mRNA abundance in HP (on the y axis) and in total RNA (on the x axis) shows the distribution of mRNAs colored by regulatory mode (Figure 3B). The anota2seq results for each comparison are presented in Table S2. Briefly, the anota2seq algorithm assigned 5.34%, 6.70%, 5.30%, and 5.00% of mRNAs to the regulatory mode translation for each comparison between control D0 and D12 STD and D12 HC3X or D20 STD and D20 HC3X differentiated cells, respectively. While less than 1% of transcripts were assigned to the buffering group, approximately 50% of transcripts were assigned to the abundance group throughout the different comparisons. These results confirm that both differentiation protocols used are accompanied by a major transcriptional rewiring, while some transcripts undergo translational regulation potentially affecting proteome remodeling.

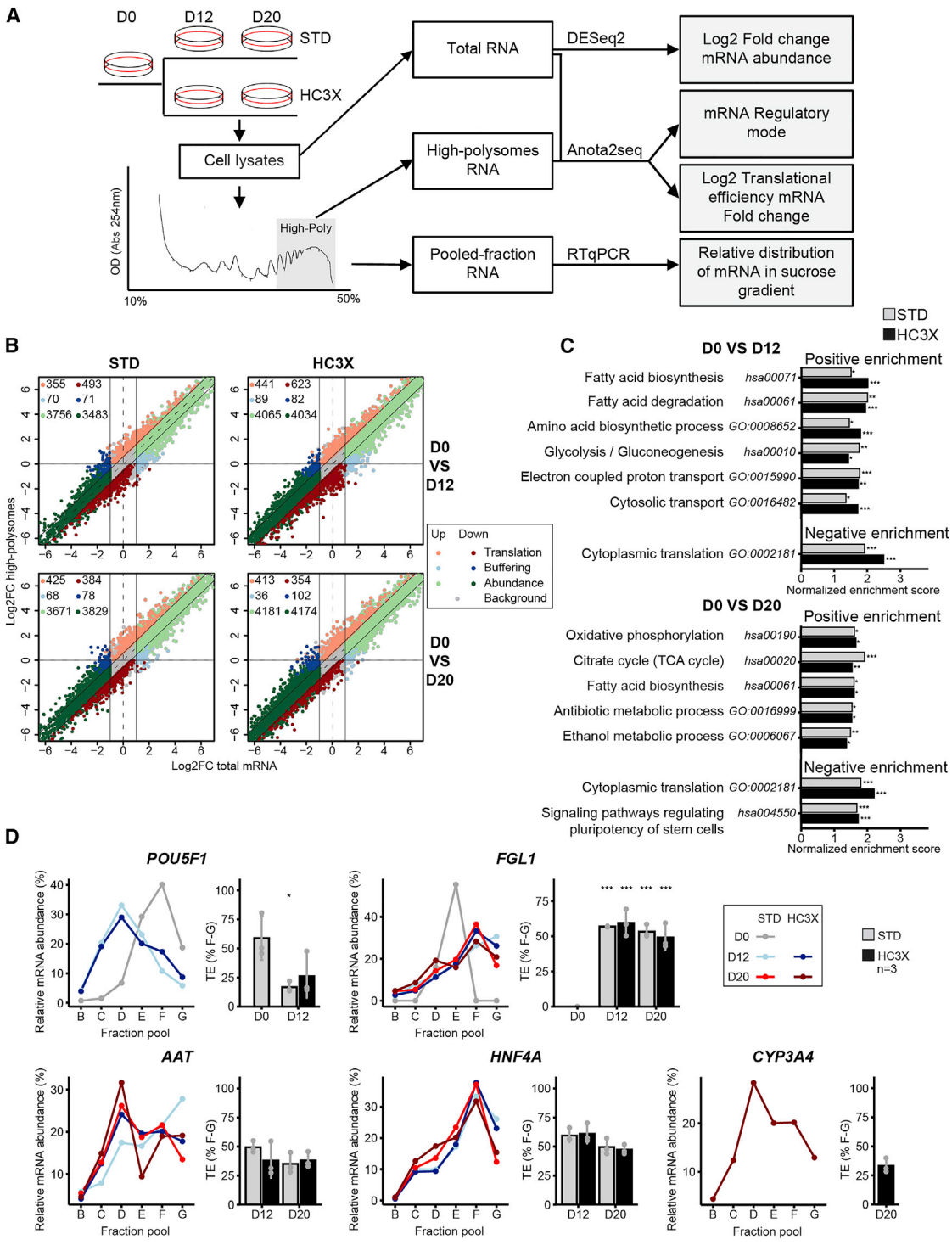

Figure 3. Characterization of translational regulation during differentiation

(A) Schematic workflow of polysome profiling experiment. Cell lysates from control D0 and differentiating cells were loaded on a sucrose density gradient prior to ultracentrifugation and fractionation. Measurement of 254 nm absorbance allows us to identify HP-containing fractions (polysomes with >3 ribosomes). For each experimental condition, total RNA and HP RNA samples were extracted (from cell lysate and HP fractions, respectively) and analyzed by RNA sequencing. DESeq2 analysis of total RNA samples identifies differentially expressed genes, while anota2seq analysis identifies differentially translated genes during differentiation. Equal volumes of fractions were pooled

(legend continued on next page)

To analyze these results more in depth, GSEA using the GO biological process and KEGG annotation databases was performed on the transcript list ranked on Log2TE FC for each comparison (see complete list of results in Table S3). D0 control cell comparisons with differentiating cells at D12 highlighted several groups of positively enriched terms linked to metabolism (Figure 3C), including fatty acid, amino acid, glucose and energy metabolism, and terms related to cellular transport.

Among the negatively enriched terms, we found a significant number of terms related to protein synthesis and translation, as previously observed in the proteomic GSEA (Figures 1D and 1E). These observations support a strong contribution of translational regulation to the downregulation of protein abundance involved in the translational machinery. Comparing D0 control cells with D20 differentiated cells from the STD or HC3X protocol (Figure 3C), numerous metabolism-related terms (associated with fatty acid and oxidative phosphorylation (OXPHOS) metabolism) were again observed, as well as some terms more specifically associated with hepatogenic differentiation such as cellular detoxification. Translation-associated terms were also strongly negatively enriched comparing D0 and D20 differentiating cells. These results indicate that translational regulation may contribute to the metabolic maturation occurring during hepatogenic differentiation but is also involved in the reduction of translation-related protein synthesis observed in the proteomic dataset.

It is important to emphasize that a significant number of hepatospecific transcripts were excluded from anota2seq analysis. Indeed, calculation of TE FC requires the comparison of the enrichment of a transcript in HP fractions with total RNA in both compared experimental conditions. However, several hepatospecific transcripts were not detected in HP fractions of D0 control iPSCs, preventing the anota2seq algorithm from calculating the Log2TE FC for these transcripts. Indeed, when raw count results for a group of 40 transcripts commonly used as hepatocyte differentiation markers (Zabulica et al., 2019) were retrieved, about half of the candidates (52.5%) presented 0 counts in at least one sample, excluding them from the analysis (data not shown). We thus combined overrepresentation analysis (ORA) using the Gene Ontology Biological Process (GOBP) and KEGG databases and manual scanning of the translation set of genes to find relevant candidates regulated at the translational level. This allowed identification of different mRNAs encoding proteins involved in endodermal lineage differentiation, such as hepatocyte nuclear factor 1B (*HNF1B*; Log2FC TE of 0.96 and 0.88 for STD and HC3X protocols) or β-catenin (*CTNNB1*; Log2FC TE of 0.61 and 0.74 for STD and HC3X protocols), as translationally upregulated in D0 versus D12 comparisons.

Interestingly, the key pluripotency gene *POU5F1*, while strongly downregulated at the mRNA level during differentiation (see Figure 1C), was also assigned to the translation group for the D0 versus D12 comparison with Log2FC TE of −1.26 and −0.67 for the STD and HC3X protocols. The distribution profile of *POU5F1* transcripts in sucrose gradient obtained by qRT-PCR (Figure 3D) showed enrichment in HP fractions (fractions F-G) in the D0 condition, while its distribution shifted toward non-polysomal fractions in D12 differentiated cells. This confirms that *POU5F1* mRNA presents decreased translation efficiency during differentiation, as previously described (Tahmasebi et al., 2016). For D0 versus D20 comparisons, anota2seq analysis classified several genes involved in cellular detoxification in the translation group, including alcohol dehydrogenase 6 (*ADH6*; with Log2TE FC of 1.56 and 1.25) and aldehyde dehydrogenase family 3 member B1 (*ALDH3B1*; with Log2TE FC of 2.56 and 2.49). Finally, the hepatokine hepassocin (also known as fibrinogen-like protein 1, *FGL1*) was identified as translationally regulated in all

three by three prior to RNA extraction of eight pooled fractions (A to H) covering the sucrose gradient. Pooled RNA fractions were analyzed by qRT-PCR to validate translationally regulated candidates.

(B) Scatterplot of Log2FC mRNA abundance in HP (x axis) and total (y axis) mRNA samples for control D0 iPSCs versus differentiating cells at D12 and D20 with the STD or HC3X differentiation protocol. Genes are classified by regulatory mode: translation (orange) for genes whose translational regulation is expected to have an impact on protein level, buffering (blue) for genes whose translational regulation is opposite to transcriptional regulation, mRNA abundance (green) for genes regulated at the transcriptional level, and background (gray) for genes not regulated at the translational nor transcriptional level. For each regulatory mode, dark colors indicate upregulation and light colors indicate downregulation.

(C) Ontology analysis of polysome profiling data comparing control and differentiated cells by GSEA of the Log2TE FC ranked gene list using the GO biological process and KEGG annotation databases. Results are shown for several hepatocyte differentiation-relevant terms and expressed as normalized enrichment score (terms with $p < 0.05$ were considered significantly enriched). *$p < 0.05$, **$p < 0.01$, and ***$p < 0.001$.

(D) qRT-PCR analysis of hepatic transcripts of the "translation group" (*POU5F1*, *HNF1B*, and *FGL1*) and key hepatic genes (*HNF4A*, *AAT*, and *CYP3A4*) showing the relative distribution of mRNAs in pooled fractions of the sucrose density gradient. Pooled fractions B-C-D and F-G correspond to subpolysomal and HP fractions, respectively. Results are normalized by a spiked-in exogenous luciferase RNA and expressed as mean of percentage mRNA abundance in the fraction from three independent biological replicates. Boxplots represent mean ± SD TE corresponding to mRNA abundance in HP fractions (F-G). Statistical significance was calculated by ANOVA and Tukey HSD *post hoc* test.

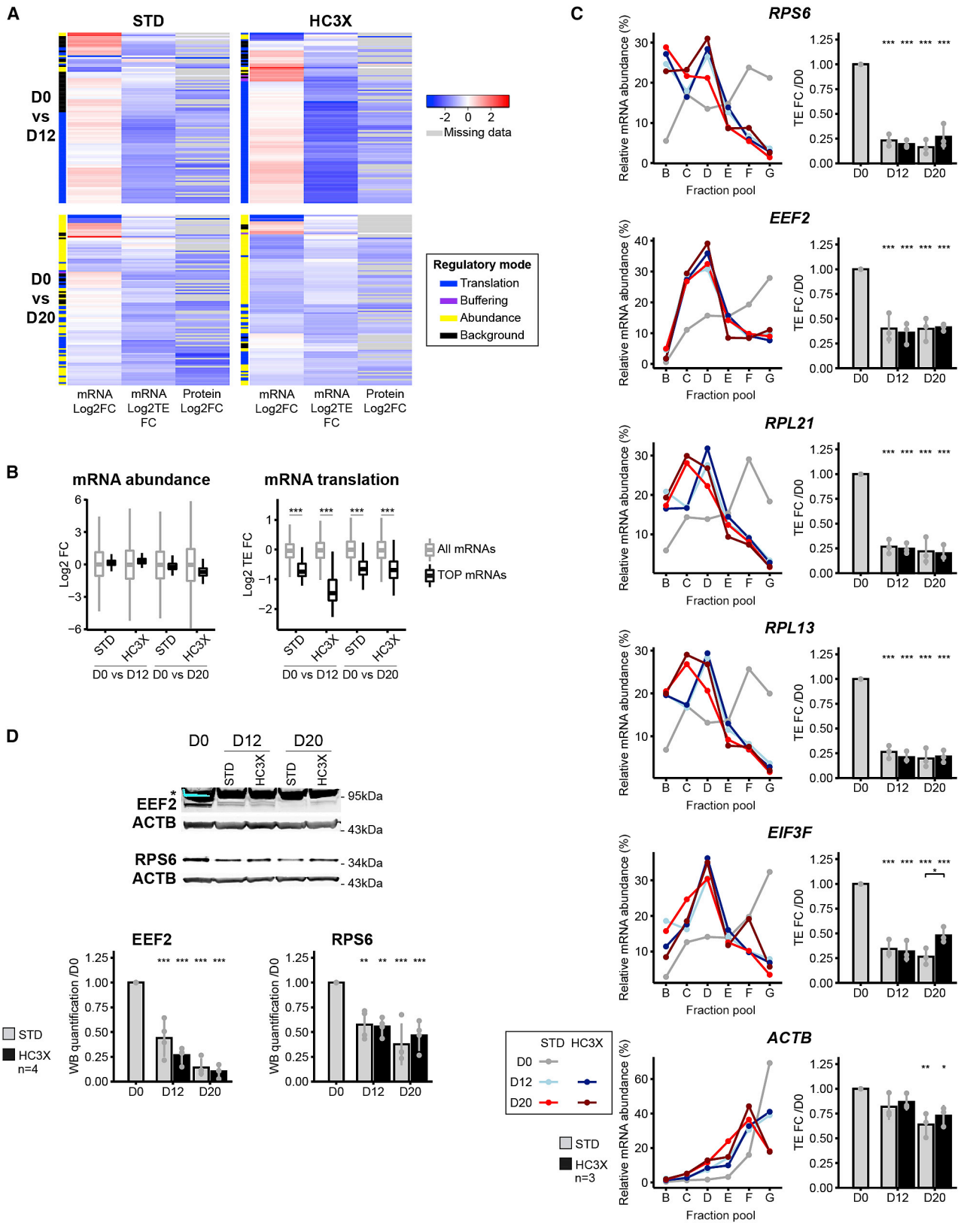

(legend on next page)

differentiating conditions (with Log2TE FC of 1.26, 1.77, 1.22, and 1.08 for D12 STD, D12 HC3X, D20 STD, and D20 HC3X, respectively). *FGL1* mRNA distribution over the sucrose gradient also confirmed the induction of mRNA translation as shown by the recruitment of *FGL1* mRNA in HP-containing fractions in differentiating cells (Figure 3D).

Next, we assessed the qRT-PCR-based TE of key hepatic markers excluded from anota2seq analysis in differentiated cells to evaluate how efficiently these genes were translated during differentiation. The mRNA distribution profile of hepatocyte transcription factors *HNF4A* and *AAT* showed consistent TE with approximately 50% of mRNA in HP fractions of differentiating cells in all conditions (Figure 3D). The *CYP3A4* mRNA profile at D20 after the HC3X protocol (the only condition expressing a sufficient amount of mRNA) showed a rather modest TE with approximatively a third of mRNA distribution in HP fractions.

Altogether, the characterization of specific translational regulation occurring during hepatogenic differentiation supports a global contribution of translational regulation to metabolic maturation of differentiating cells. In addition, while differentiating cells undergo a global decrease in protein synthesis, several transcripts involved in hepato-specific differentiation show translational upregulation, while different hepatocyte-specific markers were shown to be efficiently translated in differentiated cells.

Translation of TOP mRNAs is decreased upon hepatogenic differentiation

Our results showed that numerous proteins involved in translation are less abundant during differentiation, while mRNAs encoding those proteins are less efficiently translated. mRNAs encoding ribosomal proteins and several translational factors, such as those involved in initiation and elongation, display a terminal oligopyrimidine tract (TOP) sequence in their 5′ UTR, allowing the control of their translation (Avni et al., 1996; Jefferies et al., 1994). Thus, we hypothesized that translation of TOP mRNAs may be specifically repressed during hepatogenic differentiation. A core set of TOP mRNAs has recently been defined (Philippe et al., 2020). For these transcripts, the heatmaps of transcriptomic (Log2FC), translatomic (Log2TE FC), and proteomic (Log2FC) results associated with anota2seq regulatory modes are presented (Figure 4A).

Our proteomic results confirmed the global downregulation of TOP mRNA-encoded proteins during hepatogenic differentiation, while at the transcript level, TOP mRNAs were not significantly downregulated during hepatogenic differentiation (Figure 4B). Finally, polysome profiling results confirmed the global decrease in TOP mRNAs TE during differentiation at all time points, as confirmed by their mean Log2TE FC (Figure 4B). Thereby, anota2seq analysis massively assigned TOP mRNAs to the translation group at D12 for both protocols. For hepatic maturation time points, the superposition of transcriptional repression onto the reduction of translational efficiency shifted many transcripts in the abundance group, while a significant number of TOP mRNAs remained in the translation group. These results show that translational repression of TOP mRNAs may be an important driver of the decrease in ribosomal protein abundance observed during differentiation.

We next selected several TOP mRNA candidates (*RPS6*, *EEF2*, *RPL21*, *RPL13*, and *EIF3F*) to validate the translatomic results by qRT-PCR analysis of pooled fractions from the gradient (Figure 4C). All the TOP mRNAs selected presented a distribution profile enriched in HP fractions (fractions F-G on the graphs) in D0 control iPSCs. However, TOP mRNAs clearly shifted toward non-polysomal fractions upon hepatogenic differentiation. Calculating a qRT-PCR-based FC TE by comparing the percentage of mRNA abundance in fractions F-G confirmed at least a 2-fold decrease in TE for all TOP mRNAs studied upon differentiation, confirming their translational repression.

Figure 4. Translation of TOP mRNAs is decreased upon hepatogenic differentiation

(A) Heatmaps of omics results of core TOP mRNAs on differentiating versus control D0 iPSCs. For each comparison, results are expressed as transcriptomic Log2FC (mRNA abundance), Log2TE FC (mRNA translation), and proteomic Log2FC (protein abundance) (for first, second, and third columns, respectively). Labels correspond to regulatory mode obtained by anota2seq (gray corresponds to missing values from proteomic dataset).

(B) Boxplots of mean Log2FC (mRNA abundance) and Log2TE FC (mRNA translation) of core TOP mRNAs or all analyzed mRNAs for D0 versus differentiating cells. Statistical significance was calculated by ANOVA and Tukey's HSD *post hoc* test.

(C) qRT-PCR analysis of TOP mRNA candidates showing the relative distribution of mRNAs in pooled fractions of sucrose density gradient. Pooled fractions B-C-D and F-G correspond to subpolysomal and high-polysomal fractions, respectively. Results are normalized by a spiked-in exogenous luciferase RNA and expressed as mean of percentage mRNA abundance in the fraction from three independent biological replicates. Boxplots represent mean ± SD TE FC corresponding to fold change in mRNA abundance in high-polysome (F-G) fractions relative to control iPSCs at D0. Statistical significance was calculated by ANOVA and Tukey's HSD *post hoc* test.

(D) Western blot analysis of TOP mRNA-encoded proteins RPS6 and EEF2 (* indicates non-specific signal). Graphs show quantification of western blot signals normalized to ACTB and expressed as mean ± SD of fold change over D0 at D12 and D20 with STD and HC3X protocols. Statistical significance was calculated by ANOVA and Tukey's HSD *post hoc* test. *$p < 0.05$, **$p < 0.01$, and ***$p < 0.001$. See also Figure S1.

Finally, western blot analysis of RPS6 and EEF2 confirmed the progressive downregulation of protein abundance during hepatogenic differentiation (Figure 4D).

TOP mRNA translation is largely considered as regulated by the mammalian target of rapamycin (mTORC1)/LA-related protein 1 (LARP1) regulatory axis (Berman et al., 2020). Strikingly, western blot analysis demonstrated that the abundance of LARP1 is progressively decreased during hepatogenic differentiation (Figure S1A). In addition, detecting mTOR and P-mTOR (S2448, indicative of mTORC1 activation) protein abundance together with phosphorylation status of its targets, EIF4E-binding protein 1 (4EBP1), P70 S6 kinase (S6K1), and S6K1 target ribosomal protein S6 (RPS6), indicated that mTORC1 is not activated during hepatogenic differentiation (Figure S1B). Finally, other proteins involved in the control of TOP mRNAs translation include eukaryotic initiation factor 4G1 (EIF4G1) (Thoreen et al., 2012). Interestingly, western blot analysis of EIF4G1 protein abundance showed a strong decrease upon hepatogenic differentiation with both STD and HC3X protocols. Whether LARP1 and/or EIF4G1 plays a role in the control of TOP mRNA translation during hepatogenic differentiation will require further investigation.

In conclusion, our results show that TOP mRNAs are globally less efficiently translated during hepatogenic differentiation, while their mRNA abundance is also downregulated during hepatogenic maturation. This argues that the downregulation of protein abundance of the translation machinery is controlled first at the translational level during hepatogenic differentiation, while it is progressively repressed at the transcriptional level.

DISCUSSION

In this study, using two iPSC differentiation protocols, we characterized in great detail a global downregulation of protein synthesis during hepatogenic maturation. This observation was somehow unexpected, considering that: (1) hepatocytes represent "metabolic factories" involved in protein, carbohydrate, and lipid metabolism and are characterized by a high metabolic rate; (2) several lines of evidence support that PSCs maintain a low basal translation rate (Tahmasebi et al., 2019); and (3) several studies have demonstrated that differentiation of PSCs induces global upregulation of protein synthesis (Easley et al., 2010; Guzzi et al., 2018; Sampath et al., 2008). However, we demonstrated that protein synthesis regulation followed a two-step mode wherein early events of pluripotency exit are accompanied by a global transient upregulation of protein synthesis, while a later cell maturation step induces translational repression. Interestingly, some other examples of more advanced differentiation protocols that also yield decreased global protein synthesis are described in the literature. This is the case for cardiomyocytes and neural differentiation (Baser et al., 2019; Pereira et al., 2019). This supports a revisited model of global translational regulation of stem cell differentiation where the activation of the translation machinery previously documented is a transient step that is not maintained throughout the complete differentiation process.

Both the proteomic and the translatomic data strongly identified the translation machinery, including many ribosomal proteins, as negatively enriched during hepatogenic differentiation. The results also highlight that translation of TOP mRNAs, encoding many ribosomal proteins and translational factors, is decreased during hepatogenic differentiation. Interestingly, pioneering work in the field of translational regulation of ribosomal proteins includes the observation of a decreased ribosome loading of mRNAs encoding ribosomal proteins in mouse adult liver compared with fetal liver, which is in agreement with our results (Aloni et al., 1992). The precise mechanism of translational control of TOP mRNAs is still debated, but LARP1 appears to be a major actor controlling TOP mRNA fate downstream of mTORC1 (Berman et al., 2020). Contradictory mechanisms of LARP1-mediated regulation of TOP mRNAs have been documented, including mRNA translational repression mediated by the binding of non-phosphorylated LARP1 to 5′ TOP sequences or, in contrast, the stabilization of TOP mRNA by LARP1 binding (Aoki et al., 2013; Tcherkezian et al., 2014; Thoreen et al., 2012). Whether the progressive decrease in LARP1 protein abundance observed during hepatogenic differentiation in the current study directly controls the translation or mRNA abundance of TOP mRNAs remains an open question, but our data suggest that such mechanism would be mTORC1 independent. Considering the scarce examples of physiological conditions that make use of LARP1-mediated regulation mechanisms, our data highlight the interest in further research on the role of this protein in cell differentiation. Finally, investigations of TOP mRNA translational control also led to the observation that RNAi-mediated depletion of eIF4G1 (the EIF4F complex scaffold protein) led to a global decrease in protein synthesis with selective TOP mRNA translational repression (Thoreen et al., 2012). Interestingly, while presenting a similar phenotype, cells undergoing hepatogenic differentiation also showed a strong decrease in EIF4G1 abundance. These results suggest that EIF4G1 should also be considered for further investigations regarding TOP mRNA translation.

Specifically, the analysis of the polysome profiling TE results showed positive enrichment of several terms associated with different metabolic pathways, including fatty acid, amino acid, and glucose metabolism; cellular

respiration; and cellular detoxification. Interestingly, similar observations have been documented in a different model of hepatogenic maturation of HepaRG immortalized hepatic progenitors (Parent and Beretta, 2008). Indeed, microarray results of polysome-bound and total mRNA of differentiating HepaRG cells showed increased polysome-bound abundance of several mRNAs encoding proteins involved in lipid and drug metabolism, such as the fatty acid synthase (*FASN*), which we also found to be differentially translated in this study. Hepatocytes are well known for their high metabolic activity involved in carbon, lipid, protein, and exogenous compounds (Liu et al., 2017). In this context, our results thus support that the global translational reprogramming occurring during hepatogenic differentiation contributes to the metabolic maturation of differentiating hepatocytes by inducing expression of the metabolic protein machinery.

Finally, regarding hepatospecific transcript translational regulation, while significant numbers of hepatospecific mRNA markers were excluded from the anota2seq analysis, GO analysis still highlighted several mRNAs encoding metabolic enzymes involved in cellular detoxification, such as *ADH6*, *ALDH3B1*, or *SULT1A2*, as being translationally regulated. Whether a common specific mechanism of translational upregulation of these candidates is involved in hepatogenic differentiation remains an interesting open question. We also characterized the translational induction of *FGL1* during hepatogenic differentiation, a hepatokine initially identified as upregulated in regenerating liver (Hara et al., 2001), which is proposed to play an autocrine role regulating different aspects of hepatocyte biology such as proliferation, liver injury protection, and lipid metabolic cross talk with adipocytes (Demchev et al., 2013; Li et al., 2010; Liu and Ukomadu, 2008). Regulation of FGL1 expression and its role in differentiation are currently not characterized, but our data suggest that translational regulation may be involved in the expression of this protein during differentiation.

In this study, we characterized the contribution of translational regulation to the proteomic remodeling occurring during iPSC hepatogenic differentiation. Based on the results, we conclude that, during hepatogenic differentiation, a global decrease in protein synthesis is accompanied by a specific translational rewiring toward hepato-specific transcripts.

EXPERIMENTAL PROCEDURES

Resources availability

Corresponding author

Further information and requests for resources and reagents should be directed to the corresponding author, Patricia Renard, at patsy.renard@unamur.be.

Materials availability

All reagents and their references are listed in Table S4. Unique materials generated in this study are available from the corresponding author with a completed Materials Transfer Agreement. Stable reagents generated in this study are available from the corresponding author without restriction.

Data and code availability

RNA-seq data are deposited in the Gene Omnibus repository under accession no. GSE173106, and mass spectrometry proteomics data have been deposited in the ProteomeXchange Consortium via the PRIDE (Perez-Riverol et al., 2022) partner repository with the dataset identifiers PXD038204 and 10.6019/PXD038204. This study did not generate any novel codes but used previously published methods.

hiPSC culture

BJ1 HC3X iPSCs wherein HNF1A, FOXA3, and PROX1 can be induced by doxycycline induction (Boon et al., 2020) were cultured on hESC qualified-Matrigel-coated vessels in mTESR PLUS medium supplemented with 1% penicillin-streptomycin. Cells were passaged every 5–6 days by Accutase detachment and plated at a 1/10 dilution. Cells were replated in medium supplemented with 10 μM ROCK inhibitor (Y27632) for the first 24 h.

Hepatogenic differentiation

The STD and HC3X hepatogenic protocols were conducted as described in Boon et al. (2020); see the supplemental information for extensive details.

Polysome profiling

The polysome profiling protocol was adapted from Gandin et al. (2014). A 2 × 150-cm plate of control or differentiating hiPSCs was incubated with 0.1 mg/mL cycloheximide for 5 min in differentiating medium. Cells were then rinsed twice in 0.1 mg/mL cycloheximide in ice-cold PBS, scraped in 500 μL polysome lysis buffer (5 mM Tris-HCl [pH 7.4], 1.5 mM KCl, 2.5 mM $MgCl_2$, 0.1 mg/mL cycloheximide, 100 U/mL RNasin, 1× EDTA-free Complete protease inhibitor cocktail, 2 mM DTT, 0.5% Triton X-100, 0.5% deoxycholate), and incubated on ice for 10 min. Lysates were cleared by centrifugation at 16,000*g* for 7 min at 4°C, and 15 OD (Abs 260 nm) was loaded on a continuous 10%–50% sucrose density gradient prepared in a buffer containing 20 mM HEPES (pH 7.6), 100 mM KCl, 5 mM $MgCl_2$, 0.1 mg/mL cycloheximide, 1× EDTA-free Complete protease inhibitor cocktail, and 100 U/mL RNasin. Gradients were centrifuged at 35,000 rpm for 3 h in a SW41TI rotor at 4°C. Gradients were then fractionated into 24 fractions from the top using a Foxy Jr. fraction collector (Teledyne ISCO) with simultaneous measurement of absorbance at 254 nm using a UA-6 cell (Teledyne ISCO). For RNA-seq analysis, RNA was extracted from a pool of 500 μL prepared by collecting similar volumes of fractions containing HP (polysomes with >3 ribosomes) (for HP RNA) and from polysome lysates (for total RNA). For qPCR analysis, 100 μL of each fraction was pooled three by three to generate eight pooled fractions. Pooled fractions were spiked with 1 ng of *Renilla* luciferase RNA prior to RNA extractions and reverse transcription (RT) using GoScript reverse transcriptase with random primers (Promega A2791). A ReliaPrep RNA Miniprep

Table 1. List of qRT-PCR primers

Gene	Forward primer	Reverse primer	Source
HNF1a	ACACCTCAACAAGGGCACTC	TGGTAGCTCATCACCTGTGG	Boon et al., 2020
FOXA3	ATTCTCTCTGGCATGGGTTG	AAATTCCCCACACCCTAACC	
PROX1	TCACCTTATTCGGGAAGTGC	GGAGCTGGGATAACGGGTA	
GATA4	TCCAAACCAGAAAACGGAAG	CTGTGCCCGTAGTGAGATGA	
HNF4A	ACTACGGTGCCTCGAGCTGT	GGCACTGGTTCCTCTTGTCT	
AAT	AGGGCCTGAAGCTAGTGGAT	TCCTCGGTGTCCTTGACTTC	
ALB	ATGCTGAGGCAAAGGATGTC	AGCAGCAGCACGACAGAGTA	
CYP3A4	TTCCTCCCTGAAAGATTCAGC	GTTGAAGAAGTCCTCCTAAGCT	
POU5F1	ACATCAAAGCTCTGCAGAAAGAACT	CTGAATACCTTCCCAAATAGAACCC	
UBE3C	TTTCCCATTGCTAATGGCC	CTGATACAGCCATATCAAACGT	GetPrime no. 2079621
FGL1	ATTGTGACATGTCCGATGG	TTCATAGTCTTTCCATCCTCTG	GetPrime no. 1840886
RPL21	AAACATGGAGTTGTTCCTTTGG	AGTACCCATTCCCTTGATGTC	GetPrime no. 1889390
EEF2	TCTTCAAGGTGTTTGATGCG	CCAGTTTGATGTCCAGTTTCTC	GetPrime no. 1955377
RPL13	TCCGGAACGTCTATAAGAAGG	ATACGGAGACTAGCGAAGG	GetPrime no. 2087768
RPS6	GAGAATGAAGGAGGCTAAGG	GAAGTAGAAGCTCGCAGAG	GetPrime no. 1861997
EIF3F	TGCAGAGGATGTACTGTCTG	GGTACTTGGTTAACCAGGCT	GetPrime no. 1884548

System (Promega Z6010) was used for all RNA extractions by mixing samples with an equal volume of lysis buffer (LBA) prior to proceeding with the manufacturer's instructions.

Real-time qRT-PCR analysis

Total RNA samples were extracted from control and differentiating cells using the ReliaPrep RNA Miniprep System (Promega Z6010) following the manufacturer's instructions. RNA was reverse transcribed using GoScript reverse transcriptase with random primers (Promega A2791). cDNA was then analyzed by real-time qPCR using a GoTaq qPCR Master Mix (Promega, A6002) on a ViiA 7 Real-Time PCR System (Thermo Fisher). The primers used are listed in Table 1. Differentiation marker expression was calculated as relative expression normalized on the housekeeping gene UBE3C using the $2^{-\Delta Ct}$ method.

Western blot analysis

Control and differentiating cells at indicated time points were rinsed twice in ice-cold PBS prior to cell scraping in lysis buffer (20 mM Tris-HCl [pH 7.5], 150 mM NaCl, 15% glycerol, 1% Triton X-100, 2% SDS, 1× Complete protease inhibitor cocktail, 25 mM Na_3VO_4, 250 mM 4-nitrophenylphosphate, 250 mM glycerophosphate, 125 mM NaF, 0.17 U/μL Supernuclease). Lysates were incubated 10 min at 12°C with medium agitation and cleared by centrifugation at 16,000*g* for 10 min at 12°C. Protein concentration was measured in the supernatant using Pierce 660 nm Protein Assay Reagent (Thermo Fisher Scientific, 22660) according to the manufacturer's instructions. Ten to fifty micrograms of protein was resolved in NuPage 4%–12% bis-tris gels (Invitrogen, NP0321BOX) prior to transfer to a PVDF membrane. Primary antibodies and secondary infrared dye-coupled antibodies were diluted in Intercept (PBS) blocking buffer (Li-Cor Biosciences, 927-70001) prior to immunodetection using an Odyssey infrared imager (Li-Cor Biosciences). The primary antibodies used were anti-LARP1 (ab86359) and EEF2 (ab40812) from Abcam, anti-ACTB (T5168) from Sigma, anti-puromycin (MABE343) from Merck Millipore, anti-RPS6 (2217) from Cell Signaling, and anti-EIF4G1 (sc-133155) from Santa Cruz Biotechnology. Primary antibodies were used at 1:1,000 dilutions (excepted anti-ACTB, 1:20,000, and anti-puromycin, 1:5,000). Secondary antibodies were goat anti-rabbit IgG (926-32211), goat anti-mouse IgG (926-32210), and goat anti-mouse IgG (926-68070) from Li-Cor Bioscience and were used at a dilution of 1:10,000.

Puromycin-incorporation assay

Puromycin-incorporation assay (Schmidt et al., 2009) was achieved by treating cells with 5 μg/mL puromycin in culture medium for 10 min prior to lysis and western blot analysis as described under "western blot analysis" using anti-puromycin antibody. Cells left untreated or cells treated with 20 μg/mL cycloheximide 30 min before puromycin treatment were used as negative controls.

Bioinformatics analysis

For differential expression analysis of RNA-seq raw counts, comparison of gene expression between experimental conditions was made using DESeq2 with the Wald test. For translatomic analysis, TMM-Log2 transformed counts were analyzed using R

package anota2seq (Oertlin et al., 2019) with custom settings (minSlopeTranslation = −1, maxSlopeTranslation = 2, minSlopeBuffering = −2, maxSlopeBuffering = 1, maxPAdj = 0.25, selDeltaPT = log2(1.5), selDeltaTP = log2(1.5), selDeltaP = 0, selDeltaT = 0). GSEA was done on gene lists ranked on Log2DeltaPT (for translatomic results, referred to as Log2TE FC in this publication) or Log2FC (for transcriptomic and proteomic results) using R package ClusterProfiler (Yu et al., 2012). Similarly, overrepresentation analysis was done on the translation group of genes identified by anota2Seq. Heatmaps were generated using R package gplot. All analyses were made using statistical programming language R.

Statistical analysis

Unless stated otherwise, quantitative results generated from at least three independently cultivated cells at different passages (referred to as "biological replicates" in this publication) were analyzed by one-way ANOVA followed by Tukey's HSD *post hoc* test for pairwise comparisons. For each comparison, $p < 0.05$ was considered statistically significant and encoded as *$p < 0.05$, **$p < 0.01$, and ***$p < 0.001$. All calculations were made using statistical programming language R.

SUPPLEMENTAL INFORMATION

Supplemental information can be found online at https://doi.org/10.1016/j.stemcr.2022.11.020.

AUTHOR CONTRIBUTIONS

Conceptualization, M.C. and P.R.; formal analysis, M.C. and M.D.; investigation, M.C., S.M., D.D., A.M., M.G., A.F., and C.D.; writing – original draft, M.C. and P.R.; writing – review & editing, M.C., P.R., T.A., C.V., and D.L.J.L.; funding acquisition, M.C. and P.R.; resources, C.V., M.N., and E.S.; supervision, P.R., D.L.J.L., C.V., and T.A.

ACKNOWLEDGMENTS

We would like to thank Ola Larsson and Christian Oertlin (Department of Oncology-Pathology, Science for Life Laboratory, Karolinska Institutet, Stockholm, Sweden) for their help with polysome profiling data analysis and critical comments on the manuscript. We would also like to thank Ludivine Wacheul (RNA Molecular Biology, ULB, Gosselies, Belgium) and Manoj Kumar and Rob Van Rossom (Department of Development and Regeneration, Stem Cell Institute, KU Leuven, Leuven, Belgium) for their technical help in setting up of polysome profiling (L.W.) and iPSC hepatogenic differentiation (M.K. and R.V.R.). Finally, we thank Damien Coupeau (Department of Veterinary Medicine, University of Namur, Namur, Belgium) for offering us *Renilla* luciferase RNA. This work was supported by the Fonds de la Recherche Scientifique - FNRS under grant 33705060. M.C. and D.D. are the recipients of a Fonds de la Recherche dans l'Industrie et l'Agriculture (FRIA), Belgium, fellowship and M.S. is the recipient of a Fonds National de la Recherche Scientifique (FNRS), Belgium, fellowship.

CONFLICT OF INTERESTS

The authors declare no competing interests.

Received: May 19, 2021
Revised: November 18, 2022
Accepted: November 21, 2022
Published: December 22, 2022

REFERENCES

Aloni, R., Peleg, D., and Meyuhas, O. (1992). Selective translational control and nonspecific posttranscriptional regulation of ribosomal protein gene expression during development and regeneration of rat liver. Mol. Cell Biol. *12*, 2203–2212.

Aoki, K., Adachi, S., Homoto, M., Kusano, H., Koike, K., and Natsume, T. (2013). LARP1 specifically recognizes the 3′ terminus of poly(A) mRNA. FEBS Lett. *587*, 2173–2178. https://doi.org/10.1016/j.febslet.2013.05.035.

Avni, D., Biberman, Y., and Meyuhas, O. (1996). The 5′ terminal oligopyrimidine tract confers translational control on top mrnas in a cell type-and sequence context-dependent manner. Nucleic Acids Res. *25*, 995–1001. https://doi.org/10.1093/nar/25.5.995.

Baser, A., Skabkin, M., Kleber, S., Dang, Y., Gülcüler Balta, G.S., Kalamakis, G., Göpferich, M., Ibañez, D.C., Schefzik, R., Lopez, A.S., et al. (2019). Onset of differentiation is post-transcriptionally controlled in adult neural stem cells. Nature *566*, 100–104. https://doi.org/10.1038/s41586-019-0888-x.

Berman, A.J., Thoreen, C.C., Dedeic, Z., Chettle, J., Roux, P.P., and Blagden, S.P. (2020). Controversies around the function of LARP1. RNA Biol. *18*, 207–217. https://doi.org/10.1080/15476286.2020.1733787.

Boon, R., Kumar, M., Tricot, T., Elia, I., Ordovas, L., Jacobs, F., One, J., De Smedt, J., Eelen, G., Bird, M., et al. (2020). Amino acid levels determine metabolism and CYP450 function of hepatocytes and hepatoma cell lines. Nat. Commun. *11*, 1393. https://doi.org/10.1038/s41467-020-15058-6.

Demchev, V., Malana, G., Vangala, D., Stoll, J., Desai, A., Kang, H.W., Li, Y., Nayeb-Hashemi, H., Niepel, M., Cohen, D.E., et al. (2013). Targeted deletion of fibrinogen like protein 1 reveals a novel role in energy substrate utilization. PLoS One *8*, e58084. https://doi.org/10.1371/journal.pone.0058084.

Easley, C.A., Ben-Yehudah, A., Redinger, C.J., Oliver, S.L., Varum, S.T., Eisinger, V.M., Carlisle, D.L., Donovan, P.J., and Schatten, G.P. (2010). mTOR-mediated activation of p70 S6K induces differentiation of pluripotent human embryonic stem cells. Cell. Reprogram. *12*, 263–273. https://doi.org/10.1089/cell.2010.0011.

Friend, K., Brooks, H.A., Propson, N.E., Thomson, J.A., and Kimble, J. (2015). Embryonic stem cell growth factors regulate eIF2α phosphorylation. PLoS One *10*, e0139076. https://doi.org/10.1371/journal.pone.0139076.

Gabut, M., Bourdelais, F., and Durand, S. (2020). Ribosome and translational control in stem cells. Cells *9*, 497. https://doi.org/10.3390/cells9020497.

Gandin, V., Sikström, K., Alain, T., Morita, M., McLaughlan, S., Larsson, O., and Topisirovic, I. (2014). Polysome fractionation and analysis of mammalian translatomes on a genome-wide scale. J. Vis. Exp., 51455. https://doi.org/10.3791/51455.

Gérard, C., Tys, J., and Lemaigre, F.P. (2017). Gene regulatory networks in differentiation and direct reprogramming of hepatic cells. Semin. Cell Dev. Biol. *66*, 43–50. https://doi.org/10.1016/j.semcdb.2016.12.003.

Guzzi, N., Cieśla, M., Ngoc, P.C.T., Lang, S., Arora, S., Dimitriou, M., Pimková, K., Sommarin, M.N.E., Munita, R., Lubas, M., et al. (2018). Pseudouridylation of tRNA-derived fragments steers translational control in stem cells. Cell *173*, 1204–1216.e26. https://doi.org/10.1016/j.cell.2018.03.008.

Hara, H., Yoshimura, H., Uchida, S., Toyoda, Y., Aoki, M., Sakai, Y., Morimoto, S., and Shiokawa, K. (2001). Molecular cloning and functional expression analysis of a cDNA for human hepassocin, a liver-specific protein with hepatocyte mitogenic activity. Biochim. Biophys. Acta *1520*, 45–53. https://doi.org/10.1016/S0167-4781(01)00249-4.

Ingolia, N.T., Lareau, L.F., and Weissman, J.S. (2011). Ribosome profiling of mouse embryonic stem cells reveals the complexity and dynamics of mammalian proteomes. Cell *147*, 789–802. https://doi.org/10.1016/j.cell.2011.10.002.

Jefferies, H.B.J., Reinhard, C., Kozma, S.C., and Thomas, G. (1994). Rapamycin selectively represses translation of the "polypyrimidine tract" mRNA family. Proc. Natl. Sci. Acad. USA *91*, 4441–4445.

Kristensen, A.R., Gsponer, J., and Foster, L.J. (2013). Protein synthesis rate is the predominant regulator of protein expression during differentiation. Mol. Syst. Biol. *9*, 689. https://doi.org/10.1038/msb.2013.47.

Li, C.Y., Cao, C.Z., Xu, W.X., Cao, M.M., Yang, F., Dong, L., Yu, M., Zhan, Y.Q., Gao, Y.B., Li, W., et al. (2010). Recombinant human hepassocin stimulates proliferation of hepatocytes in vivo and improves survival in rats with fulminant hepatic failure. Gut *59*, 817–826. https://doi.org/10.1136/gut.2008.171124.

Liu, Z., and Ukomadu, C. (2008). Fibrinogen-like protein 1, a hepatocyte derived protein is an acute phase reactant. Biochem. Biophys. Res. Commun. *365*, 729–734. https://doi.org/10.1016/j.bbrc.2007.11.069.

Liu, X., Wang, H., Liang, X., and Roberts, M.S. (2017). Hepatic Metabolism in Liver Health and Disease (Elsevier Inc.).

Liu, Y., Beyer, A., and Aebersold, R. (2016). On the dependency of cellular protein levels on mRNA abundance. Cell *165*, 535–550. https://doi.org/10.1016/j.cell.2016.03.014.

Lu, R., Markowetz, F., Unwin, R.D., Leek, J.T., Airoldi, E.M., MacArthur, B.D., Lachmann, A., Rozov, R., Maayan, A., Boyer, L.A., et al. (2009). Systems-level dynamic analyses of fate change in murine embryonic stem cells. Nature *462*, 358–362. https://doi.org/10.1038/nature08575.

Oertlin, C., Lorent, J., Murie, C., Furic, L., Topisirovic, I., and Larsson, O. (2019). Generally applicable transcriptome-wide analysis of translation using anota2seq. Nucleic Acids Res. *47*, e70. https://doi.org/10.1093/nar/gkz223.

Parent, R., and Beretta, L. (2008). Translational control plays a prominent role in the hepatocytic differentiation of HepaRG liver progenitor cells. Genome Biol. *9*, R19. https://doi.org/10.1186/gb-2008-9-1-r19.

Pereira, I.T., Spangenberg, L., Robert, A.W., Amorín, R., Stimamiglio, M.A., Naya, H., and Dallagiovanna, B. (2019). Cardiomyogenic differentiation is fine-tuned by differential mRNA association with polysomes. BMC Genom. *20*, 219. https://doi.org/10.1186/s12864-019-5550-3.

Perez-Riverol, Y., Bai, J., Bandla, C., García-Seisdedos, D., Hewapathirana, S., Kamatchinathan, S., Kundu, D.J., Prakash, A., Frericks-Zipper, A., Eisenacher, M., et al. (2022). The PRIDE database resources in 2022: a hub for mass spectrometry-based proteomics evidences. Nucleic Acids Res. *50*, D543–D552. https://doi.org/10.1093/nar/gkab1038.

Philippe, L., van den Elzen, A.M.G., Watson, M.J., and Thoreen, C.C. (2020). Global analysis of LARP1 translation targets reveals tunable and dynamic features of 5′ TOP motifs. Proc. Natl. Acad. Sci. USA *117*, 5319–5328. https://doi.org/10.1073/pnas.1912864117.

Roelandt, P., Vanhove, J., and Verfaillie, C. (2013). Directed differentiation of pluripotent stem cells to functional hepatocytes. Methods Mol. Biol. *997*, 141–147.

Sampath, P., Pritchard, D.K., Pabon, L., Reinecke, H., Schwartz, S.M., Morris, D.R., and Murry, C.E. (2008). A hierarchical network controls protein translation during murine embryonic stem cell self-renewal and differentiation. Cell Stem Cell *2*, 448–460. https://doi.org/10.1016/J.STEM.2008.03.013.

Schmidt, E.K., Clavarino, G., Ceppi, M., and Pierre, P. (2009). SUnSET, a nonradioactive method to monitor protein synthesis. Nat. Methods *6*, 275–277. https://doi.org/10.1038/nmeth.1314.

Schwanhäusser, B., Busse, D., Li, N., Dittmar, G., Schuchhardt, J., Wolf, J., Chen, W., and Selbach, M. (2011). Global quantification of mammalian gene expression control. Nature *473*, 337–342. https://doi.org/10.1038/nature10098.

Tahmasebi, S., Jafarnejad, S.M., Tam, I.S., Gonatopoulos-Pournatzis, T., Matta-Camacho, E., Tsukumo, Y., Yanagiya, A., Li, W., Atlasi, Y., Caron, M., et al. (2016). Control of embryonic stem cell self-renewal and differentiation via coordinated alternative splicing and translation of YY2. Proc. Natl. Acad. Sci. USA *113*, 12360–12367. https://doi.org/10.1073/pnas.1615540113.

Tahmasebi, S., Amiri, M., and Sonenberg, N. (2019). Translational control in stem cells. Front. Genet. *9*, 709. https://doi.org/10.3389/fgene.2018.00709.

Tcherkezian, J., Cargnello, M., Romeo, Y., Huttlin, E.L., Lavoie, G., Gygi, S.P., and Roux, P.P. (2014). Proteomic analysis of cap-dependent translation identifies LARP1 as a key regulator of 5′TOP mRNA translation. Genes Dev. *28*, 357–371. https://doi.org/10.1101/gad.231407.113.

Thoreen, C.C., Chantranupong, L., Keys, H.R., Wang, T., Gray, N.S., and Sabatini, D.M. (2012). A unifying model for mTORC1-mediated regulation of mRNA translation. Nature *485*, 109–113. https://doi.org/10.1038/nature11083.

Tricot, T., Helsen, N., Kaptein, S.J.F., Neyts, J., and Verfaillie, C.M. (2018). Human stem cell-derived hepatocyte-like cells support Zika virus replication and provide a relevant model to assess the efficacy of potential antivirals. PLoS One *13*, e0209097. https://doi.org/10.1371/journal.pone.0209097.

Vogel, C., and Marcotte, E.M. (2012). Insights into the regulation of protein abundance from proteomic and transcriptomic analyses. Nat. Rev. Genet. *13*, 227–232. https://doi.org/10.1038/nrg3185.

Woolnough, J.L., Atwood, B.L., Liu, Z., Zhao, R., and Giles, K.E. (2016). The regulation of rRNA gene transcription during directed differentiation of human embryonic stem cells. PLoS One *11*, e0157276. https://doi.org/10.1371/journal.pone.0157276.

You, K.T., Park, J., and Kim, V.N. (2015). Role of the small subunit processome in the maintenance of pluripotent stem cells. Genes Dev. *29*, 2004–2009. https://doi.org/10.1101/gad.267112.115.

Yu, G., Wang, L.-G., Han, Y., and He, Q.-Y. (2012). clusterProfiler: an R Package for comparing biological themes among gene clusters. Omi. A J. Integr. Biol. *16*, 284–287. https://doi.org/10.1089/omi.2011.0118.

Zabulica, M., Srinivasan, R.C., Vosough, M., Hammarstedt, C., Wu, T., Gramignoli, R., Ellis, E., Kannisto, K., Collin de l'Hortet, A., Takeishi, K., et al. (2019). Guide to the assessment of mature liver gene expression in stem cell-derived hepatocytes. Stem Cells Dev. *28*, 907–919. https://doi.org/10.1089/scd.2019.0064.

Zeevaert, K., Elsafi Mabrouk, M.H., Wagner, W., and Goetzke, R. (2020). Cell mechanics in embryoid bodies. Cells *9*, E2270. https://doi.org/10.3390/cells9102270.